



ISSN 1110-0451



(E S N S A)

Efficient Evaluation of Heat Exchangers Behaviour in Nuclear Power Plants

Elsayed H. Ali* and H. Kasban

Engineering Department, Nuclear Research Center, Atomic Energy Authority, Egypt

ARTICLE INFO

Article history:

Received: 1st Aug. 2020Accepted: 2nd Mar. 2021

Keywords:

Nuclear Power Plant,
Heat Exchanger,
Heat Transfer,
Explicit Solution.

ABSTRACT

This paper studies the performance of the primary and secondary flow paths of the heat exchangers (HEXs) in the Nuclear Power Plants (NPPs). Explicit solutions for the wall temperature, primary and secondary wall temperatures of the HEX are presented. Therefore, closed form expressions for wall temperature, primary and secondary wall temperature are proposed. Moreover, performance analysis of HEX is investigated. The various effects of pipe wall heat capacities, perimeter, fluid heat transfer (HT) coefficient and wall HT coefficient on the HEX are evaluated. The obtained results confirm that the surface contact between the two fluid passes reduces the temperature to some extent at 5 seconds. As a final point of observation, the temperature distributions through the HEX structure increases with the decrease of its perimeter. The proposed work allows more control of the HT process within the HEX. Consequently, the performance of NPPs can be improved.

1- INTRODUCTION

Energy is the main engine for social development and environmental protection around the world. Electric energy is one of the main and strategic goals of all countries. One of the main components of the NPP is the HEX which is subjected to work under complicated conditions such as: variation in pressure and a very high temperature. HEX has many types, sizes, configurations, and different flow arrangements according to its use and application. HEX can be classified among others in accordance with the transfer process or the number of fluids. The shell and tube of HEX is considered the most common type of heat transfer equipment used in industry, if it is desirable to operate under a high level pressure. For an optimum, safe and economic design, the most favorable conditions should be chosen. HEX is an essential component of the NPP, where it links between the reactor and the turbine and it is called the steam generator in many topics. In NPPs, water is pumped for collecting the heat energy produced by the chain reaction produces [1]. In the HEX, the water coming from the reactor gives up the energy to a cooler water flowing in another closed loop, then turning it into the steam through two unconnected loops of water.[2, 3]. The

Schematic of a typical boiling water reactor system (BWR) is shown in Fig.1[4, 5].

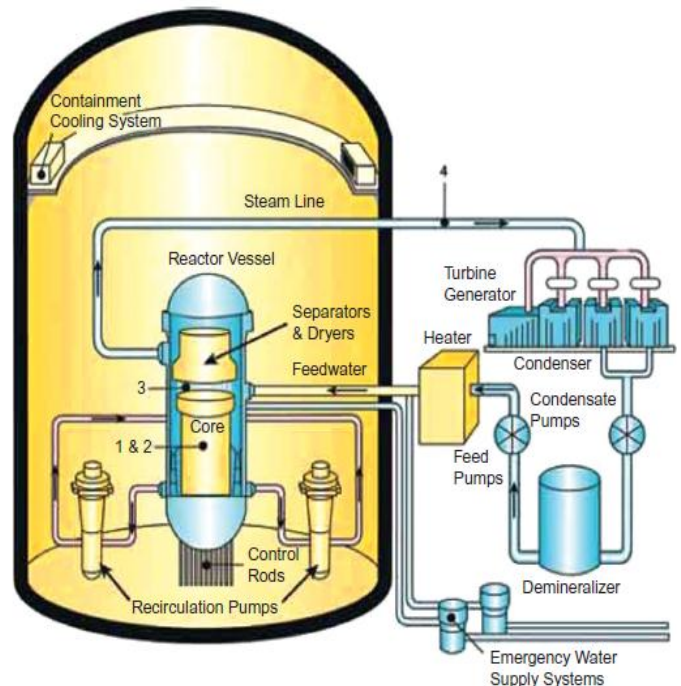


Fig. (1): Schematic of a typical boiling water reactor system

The HEX is mainly composed of the main shell containing a huge amount of tubes. Nowadays, due to modern and advanced control system strategy, the NPP can share in the electric grid with conventional power plants to meet the changes in the demand of the daily load of electricity. Therefore, the changing rate in the steam supply system becomes very high, that causes thermal stress and thermal shocks, which have a negative effect on the tubes of HEX. This paper studies and analyzes the thermal hydraulic change rate effect on the wall tubes of HEX.

Several previous studies focused on the thermal hydraulic and design of HEX. Rabbo et. al presented the metal tube mechanical properties which are too important during the design of NPP[6]. Lovász and Boros studied the great effectiveness of HEX on the performance of NPP after the accident in Fukushima and explained the heat exchange process inside the reactor containment, and developed a model containment at different simulations[7]. They studied the feedwater of HEX at high pressure with detailed structures based on a number of control volumes. They also studied the flow calculations and thermal dynamics in HEX under high pressure. Huang et. al studied the frequent degradation and effecting of wall tubes of HEX to thermal shocks due to fluid passing over the tubes[8]. The results of this study proved that the instability in temperature and dynamic flow with high temperatures have a negative effect on the NPP performance and the fluctuations in the dynamic flow instability inside the tubes have significant bad effect on cooling medium inside the HEX. Ilyas and Aydogan studied the two-phase flow through the tubes of the steam generator and investigated the pressure drop and thermal heat characteristics under various flow regimes[9].

Abed investigated the dissipation of the heat intensity from the outer surface of HEX due to natural circulation and it was very low, they found that the heat removal intensity completely depends on the surrounding ambient air temperature. The results explained that the existence of dispersed water occurs due to HT[10]. Zohuri studied the effect of hot water that contain radionuclide inside the tubes on the HEX efficiency, The author concluded that the hat pipe is the device that collects each of phase transitions and thermal conductivity[11]. Inman presented a design for a high temperature gas-cooled reactor and studied the stored heat energy inside the reactor and it can be efficiently used for electricity generation. He concluded that the chosen of metal tube depend on the desired value of stored heat energy[12].

Liu et. al concentrated mainly on the mechanism of the external heat of the HEX tube with the surrounding media in generation III of NPPs. The external HT of metal tube is analyzed. The study concludes that the HT inside the HEX is a complicated process[13]. Tashakor et. al studied the effect of existence of impurities with different concentrations inside the HEX tubes in NPP. They solved the diffusion equation of the liquid phase using the method of finite volume. The results show that the impurities have effects on thermohydraulic performance of HEX and the corrosion intensity is increased inside the tube. The highest concentration of impurities was found to exist in the regions of high temperature [15]. Xie et. al studied the characteristics of HEX heat pipe, stability, volume heat capacity and reliability on removing process of the residual heat from the reactor core[1]. The residual heat must be removed from the reactor core after shutdown. Based on the finite volume method they discussed three factors affecting on turbulent flow and HT, (1) fluid velocity, (2) pipe bundle arrangement, (3) number of rows in the fluid flow direction.

Ayodeji and Liu studied flow and HT of supercritical water in supercritical boiler water and they investigated the wall tube with numerical simulation and they found that, the HT coefficient increases by increasing the inlet flow rate[14]. Bae et. al concentrated on validation of HT condensation in nuclear reactor passive cooling system. They built and simulated a model for a single tube as a prototype to test the condensation of HT of HEX. The results indicated that the tube degradation takes place with time due to thermal effect, since the non-condensable gas concentration increased due to an accumulation around the inside tubes[14]. Cai et. al concentrated on improving the tube metal properties of the steam generator in NPP. They studied the fretting HT of the tubes[15].

Hao et. al focused on thermal resistance generation and simulation the HEX tubes based on inlet difference temperature and they proved that the rate of HT decreased and increased in the pressure inlet [20]. Talebi and Norouzi concentrated on improving the NPP performance via thermodynamic optimization. The study made a link between fossil power plant and NPP (called hybrid plant) and they evaluated its performance[16].

Torre et. al focused on the evaluation of the external structure design effects on HEX at a very high temperature. They concluded that the temperature gradient is directly proportional to the thermal stress field[17]. Yang et. al studied the bursting failure analysis in abnormal conditions of tubes HT of HEX in NPP.

They concluded that the metallography structure, mechanical properties and chemical compositions of bursted tubes should be investigated[18]. Vourganti studied and investigated the crossflow with time delay for non-linear dynamics of HEX tubes. The results were useful in the design stage for the tubes of HEX which increase the efficient operation of NPP[2]. Mehul discussed the criteria of selection of materials alloy that works under high temperature in NPP. He concluded that, there are many shapes for tube of being suitable for design the HEX[19]. Martelli presented an experimental work for developing HEX able to remove the deposited nuclear heat in the metal liquid of dual coolant lithium lead[20]. They tested and investigated the system thermal hydraulic properties to improve the knowledge of HEX code design.

The progress in modeling tools using computer led to a great development many models for HEX design and thermal control. Many techniques have been used for modeling and optimization of the HEX design such as; Computational Fluid Dynamics(CFD)[21]. The HEX thermal control studied by Borkar et. al, they presented a model for the thermal analysis of the closed feed water heaters that can help in malfunctions detection and diagnostics of the NPP. Fernández et al. carried-out the HEX performance assessment by Mamdani based adaptive neuro fuzzy inference and dynamic fuzzy reliability modelling[22, 23]. Temperature coupling analysis between nuclear steam generators and HEX inside pressurized water reactors has been carried out by El-Tokhy et al. [24].

The performance of the primary and secondary wall temperature of the HEX is studied in the present work by presenting an explicit solutions and closed form expressions. The performance analysis investigated using many variables such as; the wall heat capacities, perimeter, and Coefficients. The following sections of this study includes the performance analysis of HEX in NPPs, the simulation results and discussion and finally the conclusions of the present study.

2- PERFORMANCE ANALYSIS OF HEX IN NPP

The HEX combines two passes with a common wall (each of length L) to make counter flow HEX as depicted in Fig. 2, with flow areas A_F and velocities that can be varied. It divides the length of HEX to different elements.

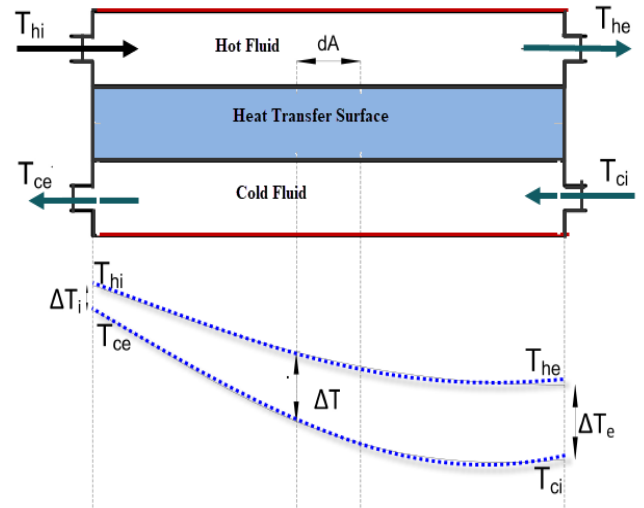


Fig. (2): Layout of HEX counter flow includes two phases[5]

The basic fluid wave equation is given by[5]:

$$\frac{dT}{dt} + V \frac{dT}{dx} = \frac{T_{wf} - T}{\tau_f} \quad (1)$$

where T , x , V , T_{wf} and τ_f denote the fluid temperature ($^{\circ}\text{F}$), the distance (ft) along flow path, the fluid velocity at t (ft/sec), the average temperature of wall section dL and the fluid HT time constant, respectively. The wall HT time constant is given by[25]:

$$\tau_w = \frac{1}{\left(\frac{1}{\tau_{ws}} + \frac{1}{\tau_{wp}}\right)} \quad (2)$$

where τ_{ws} and τ_{wp} are $\tau_{wp} = \frac{C'_w}{h_p} P$, $\tau_{ws} = \frac{C'_w}{h_s} P$,

with C'_w , P , h_s and h_p are the pipe wall heat capacities, perimeter, fluid HT coefficient and wall HT coefficient, respectively. Since, the velocity is the rate of change of distance with respect to time, Then, Eq. 1 can be rewritten as:

$$\frac{dT}{dt} + V \frac{dT}{dt} \frac{dt}{dx} = \frac{T_{wf} - T}{\tau_f} \quad (3)$$

From Eq. 1 and Eq. 3 we obtain Eq. 4.

$$\frac{dT}{dt} + \frac{dT}{dt} = \frac{T_{wf} - T}{\tau_f} \quad (4)$$

$$2 \frac{dT}{dt} = \frac{T_{wf} - T}{\tau_f} \quad (5)$$

From Eq. 5. we divide by 2, then we obtain Eq. 6

$$\therefore \frac{dT}{dt} = \frac{T_{wf} - T}{2\tau_f} \quad (6)$$

Therefore, T_p and T_s are average fluid temperatures that are given by:

$$\frac{dT_p}{dt} = \frac{T_{wf} - T_p}{2\tau_f} \quad (7)$$

$$\frac{dT_s}{dt} = \frac{T_{wf} - T_s}{2\tau_f} \quad (8)$$

Solving Eq. 7 and Eq. 8 with respect to the initial conditions $T_p(0) = T_{p0}$ and $T_s(0) = T_{s0}$. Hence, the expression for T_p and T_s were deduced that simplified and rewritten as follows:

$$T_p = T_{wf} + (T_{p0} - T_{wf}) e^{-\frac{t}{2\tau_f}} \quad (9)$$

$$T_s = T_{wf} + (T_{s0} - T_{wf}) e^{-\frac{t}{2\tau_f}} \quad (10)$$

The basic equation for the wall is given by the following equation:

$$\tau_w \frac{dT_w}{dt} + T_w = \tau_w \left(\frac{T_p}{\tau_{wp}} + \frac{T_s}{\tau_{ws}} \right) \quad (11)$$

Equation (11) can be arranged and presented as:

$$\frac{dT_w}{dt} = \left(\frac{T_p}{\tau_{wp}} + \frac{T_s}{\tau_{ws}} \right) - \frac{T_w}{\tau_w} \quad (12)$$

By solving Eq. 12 using the initial conditions, $T_w(0) = T_{w0}$, an equation for the wall temperature was deduced as follows:

$$T_w = \frac{\tau_w T_p}{\tau_{wp}} + \frac{\tau_w T_s}{\tau_{ws}} + e^{-\frac{t}{\tau_w}} \left(T_{w0} - \frac{\tau_w T_p}{\tau_{wp}} - \frac{\tau_w T_s}{\tau_{ws}} \right) \quad (13)$$

A formula for the wall temperature is reduced by substitution from Eqs. (9-10) in Eq. (12) as:

$$T_w = \left(\frac{h_p}{\chi C_w' P} \left(T_{wf} + e^{-\frac{t}{2\tau_f}} (T_{p0} - T_{wf}) \right) + \frac{h_s}{\chi C_w' P} \left(T_{wf} + e^{-\frac{t}{2\tau_f}} (T_{s0} - T_{wf}) \right) + e^{-\left(\frac{h_p}{C_w' P} + \frac{h_s}{C_w' P}\right)t} \times \left(T_{w0} - \frac{h_p}{\chi C_w' P} \left(T_{wf} + e^{-\frac{t}{2\tau_f}} (T_{p0} - T_{wf}) \right) - \frac{h_s}{\chi C_w' P} \left(T_{wf} + e^{-\frac{t}{2\tau_f}} (T_{s0} - T_{wf}) \right) \right) \right) \quad (14)$$

$$\text{where } \chi = \frac{h_p}{C_w' P} + \frac{h_s}{C_w' P}.$$

Moreover, there are two average wall section temperatures that stated as:

$$T_{ws} = T_{ws0} + (T_w - T_{w0}) \quad (15)$$

A formula for the primary wall temperature is derived and rewritten as:

$$T_{wp} = T_{wp0} - T_{w0} + \left(\left(\frac{h_p}{\chi C_w' P} \left(T_{wf} + e^{-\frac{t}{2\tau_f}} (T_{p0} - T_{wf}) \right) + \frac{h_s}{\chi C_w' P} \left(T_{wf} + e^{-\frac{t}{2\tau_f}} (T_{s0} - T_{wf}) \right) + e^{-\left(\frac{h_p}{C_w' P} + \frac{h_s}{C_w' P}\right)t} \left(T_{w0} - \frac{h_p}{\chi C_w' P} \left(T_{wf} + e^{-\frac{t}{2\tau_f}} (T_{p0} - T_{wf}) \right) - \frac{h_s}{\chi C_w' P} \left(T_{wf} + e^{-\frac{t}{2\tau_f}} (T_{s0} - T_{wf}) \right) \right) \right) \right) \quad (16)$$

Furthermore, an expression for the secondary wall temperature is presented as:

$$T_{ws} = T_{ws0} - T_{w0} + \left(\left(\frac{h_p}{\chi C_w' P} \left(T_{wf} + e^{-\frac{t}{2\tau_f}} (T_{p0} - T_{wf}) \right) + \frac{h_s}{\chi C_w' P} \left(T_{wf} + e^{-\frac{t}{2\tau_f}} (T_{s0} - T_{wf}) \right) + \right. \right. \quad (17)$$

$$\left. \left. e^{-\left(\frac{h_p}{C_w' P} + \frac{h_s}{C_w' P} \right) t} \times \left(T_{w0} - \frac{h_p}{\chi C_w' P} \left(T_{wf} + e^{-\frac{t}{2\tau_f}} (T_{p0} - T_{wf}) \right) - \frac{h_s}{\chi C_w' P} \left(T_{wf} + e^{-\frac{t}{2\tau_f}} (T_{s0} - T_{wf}) \right) \right) \right)$$

3- RESULTS AND DISCUSSION

Analytical results for the HEX model in the advanced boiling water reactor (ABWR) are performed for the main variables of interest. Fig. (3) shows the variation of wall temperature with time at various pipe wall heat capacities. The results show that the wall temperature is high at the beginning of fluid injection, then, the surface contact between the two pipes reduces the temperature to some extent at 5 seconds. Subsequently, the wall temperature is increased. However, it is limited to the pipe length and contact time. Moreover, the wall temperature increases with the pipe wall heat capacities. The Physical characteristic and the behavioral parameters of the HEX are given in table (1) and Table (2) respectively.

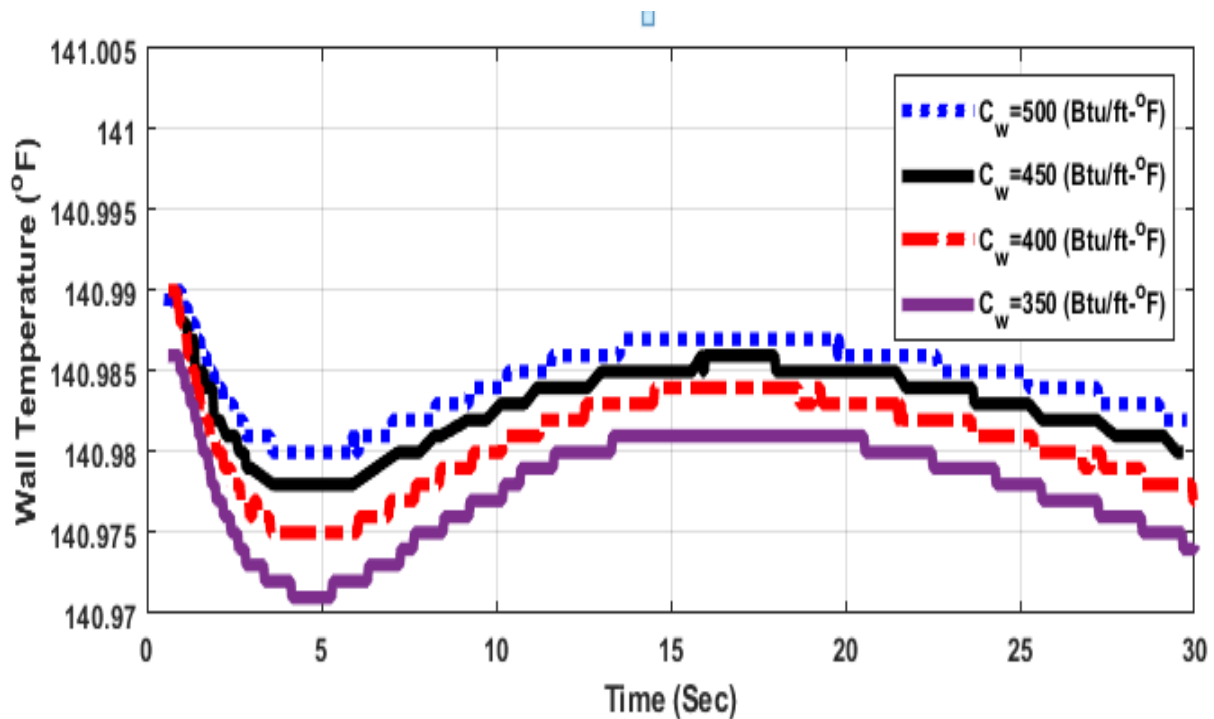
Fig. (4) shows the variation of the wall temperature with the time at various wall HT coefficients. The results show that, the final wall temperature becomes lower than its initial value, although the wall temperature depends on the initial temperature. Also, the wall temperature decreases with the wall HT coefficient. This may be due to the fact that the wall HT coefficient allows the transfer of accepted temperature to the neighboring wall pipe.

Fig. (5) illustrates the variation of the wall temperature with the time at various fluid HT coefficients. The results show that, the fluid HT coefficient conveys its temperature to the surrounding pipe wall. Consequently, the wall temperature is increased. Fig. (6) shows the variation of the wall temperature with time at various perimeters. The results show that, the wall area decreases with the decrease of the perimeter. Hence, the distributed temperature

through the HEX structure is increased. Fig. (7) shows the variation of the wall temperature with the time at various fluid HT time. The results show that, the increase of the fluid HT time reduces the distributed temperature within the pipe structure. Consequently, the wall temperature is decreased. Moreover, the obtained curves are initially started at 140.99°F. Fig. (8) shows the variation of the wall temperature with the time at various initial wall temperature. The results show that, the wall temperature is strongly affected by its initial value. Also, a rapid decrease of the wall temperature with the increase of the initial wall temperature. Fig. (9) shows the change of the primary wall temperature with the time at various perimeters. The results show that, the primary wall temperature is high at the initial time. Since, the initial wall temperature is not affected by both the input fluid and the perimeter. Then, a slow decrease in the primary wall temperature is observed with time. On other words, the primary wall temperature decreases with the perimeter. Fig. (10) depicts the variation of the primary wall temperature with the time at various fluid HT time constant. The results show that, the transferred temperature to the primary wall increases with fluid HT time constant. Fig. (11) shows the change of the secondary wall temperature with the time at various perimeters. The results show that, the HEX area increases with the perimeter. Hence, the accepted temperature through the secondary wall temperature is decreased. Fig. (12) shows the variation of the secondary wall temperature with the time at various fluid HT time constant. The results show that, the conveyed temperature increases with the fluid HT time constant. Hence, the secondary wall temperature is increased.

Table (1): Behavioral parameters and Physical characteristic of HEX in ABWR [5, 24, 26]

Length of the heat exchanger L(meter) =6.096	Fluid heat capacity/length $C'_s \left(\text{Btu}/\text{ft} - ^\circ\text{F} \right) = 500$
Flow area $A_{fs} \left(\text{ft}^2 \right) = 10$	Pipe wall heat capacity/fluid heat capacity (Primary side) $C_{ps} = 0.4$
Fluid heat transfer time constant $\tau_s \left(\text{sec} \right) = 2$	Fluid secondary side inlet temperature $t_{si} \left(^\circ\text{F} \right) = -30$
Pipe wall heat capacity/fluid heat capacity (Secondary side) $C_{ws} = 0.2$	Fluid secondary side outlet temperature $t_{so} \left(^\circ\text{F} \right) = -10$
Fluid primary side Inlet temperature $t_{pi} \left(^\circ\text{F} \right) = 40$	perimeter $P = 3.3048: 15 \text{ m}$
$C_w = 1.96: 2.8 \text{ kJ}/\text{m}^2\text{ }^\circ\text{C}$	$V_p = 1524: 6.096 \text{ m}/\text{sec}$
$T_{wo} = 60: 500 \text{ }^\circ\text{C}$	$V_s = 1524: 6.096 \text{ m}/\text{sec}$
$\tau_f = 1: 4 \text{ sec}$	$\tau_w = 2 \text{ sec}$
$\tau_{wp} = 3 \text{ sec}$	$\tau_{ws} = 3 \text{ sec}$
$h_p = 80.640: 141.12 \frac{\text{kJ}}{\text{sec}} \text{m}^2\text{ }^\circ\text{C}$	$L = 1.524: 10 \text{ m sec}$
$h_s = 80.640: 141.12 \frac{\text{kJ}}{\text{sec}} \text{m}^2\text{ }^\circ\text{C}$	

**Fig. (3): Variation of wall temperature with time at various pipe wall heat capacities**

($\tau_{ws}=3\text{sec}$, $\tau_{wp}=3\text{sec}$, $\tau_w=2\text{sec}$, $V_s=5\text{ft}/\text{sec}$).

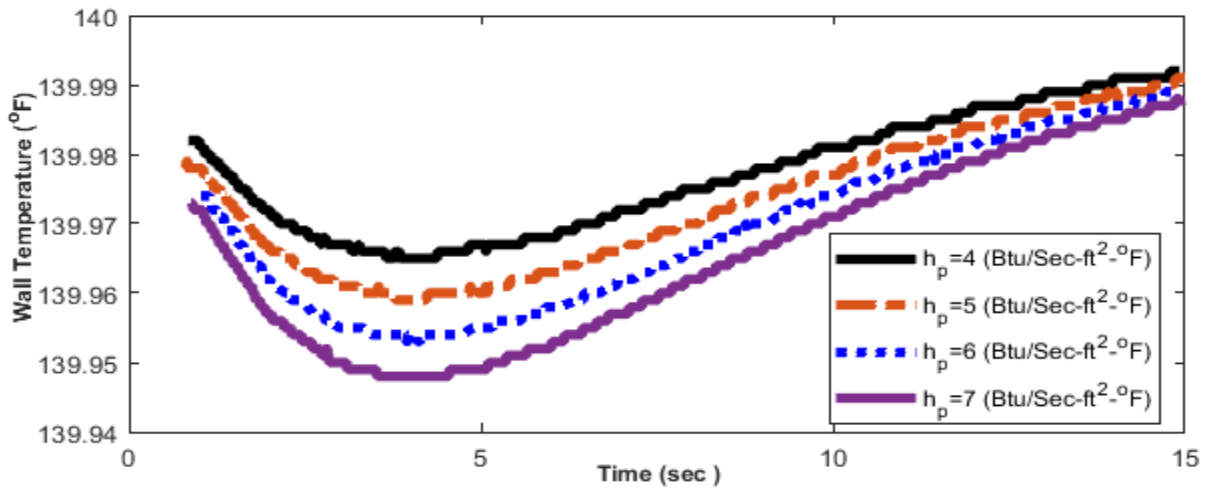


Fig.(4):Variation of wall temperature with time at various wall HT coefficient
($\tau_{ws}=3\text{sec}$, $\tau_{wp}=3\text{sec}$, $\tau_w=2\text{sec}$, $V_s=5\text{ft/sec}$).

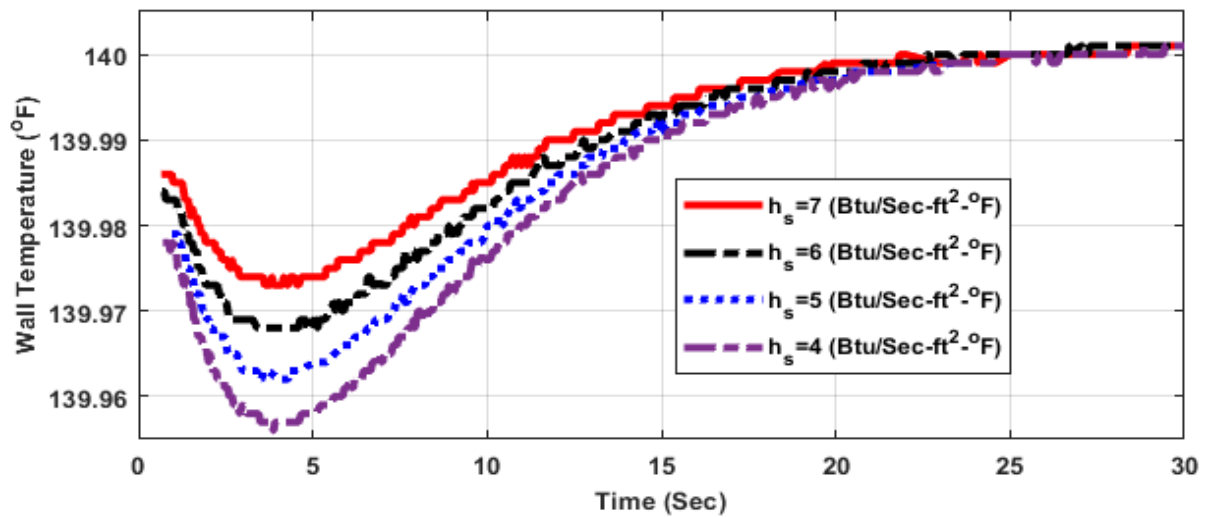


Fig. (5): Variation of wall temperature with time at various fluid HT coefficient
($\tau_{ws}=3\text{sec}$, $\tau_{wp}=3\text{sec}$, $\tau_w=2\text{sec}$, $V_s=5\text{ft/sec}$).

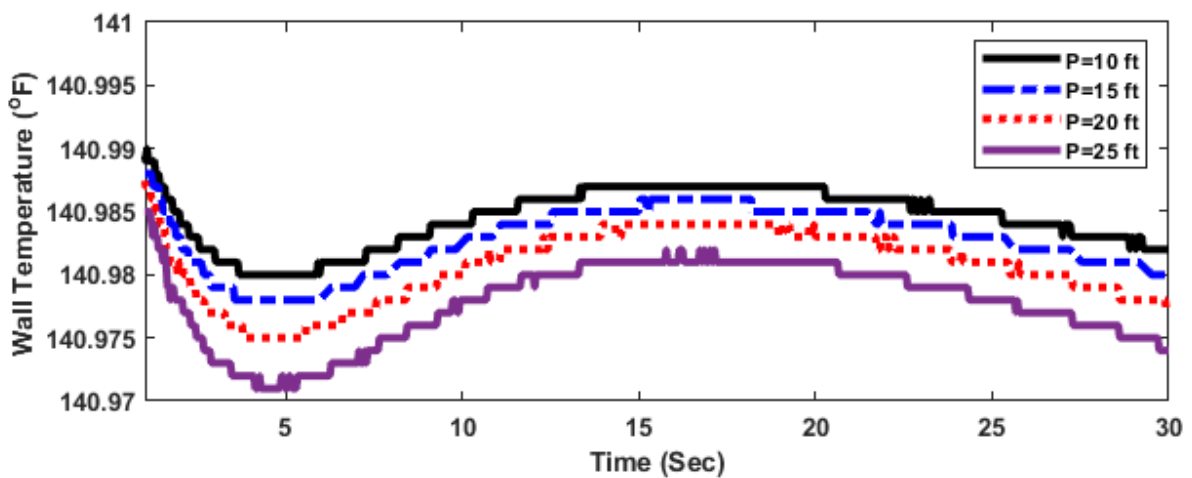


Fig. (6): Variation of wall temperature with time at various perimeter
($\tau_{ws}=3\text{sec}$, $\tau_{wp}=3\text{sec}$, $\tau_w=2\text{sec}$, $V_s=5\text{ft/sec}$).

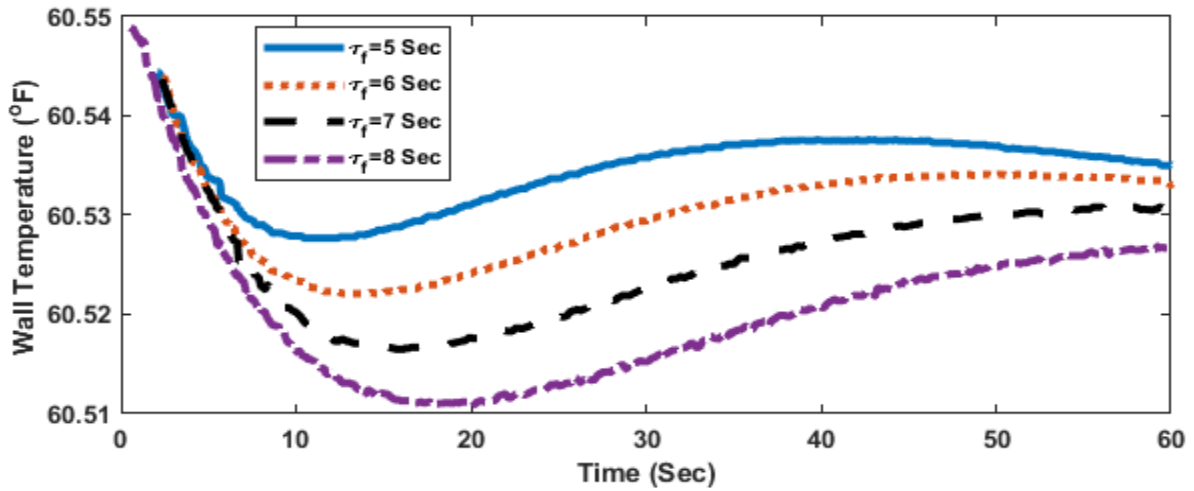


Fig. (7): Variation of wall temperature with time at various fluid HT time constant ($\tau_{ws}=3$ sec, $\tau_{wp}=3$ sec, $\tau_w=2$ sec, $V_s=5$ ft/sec).

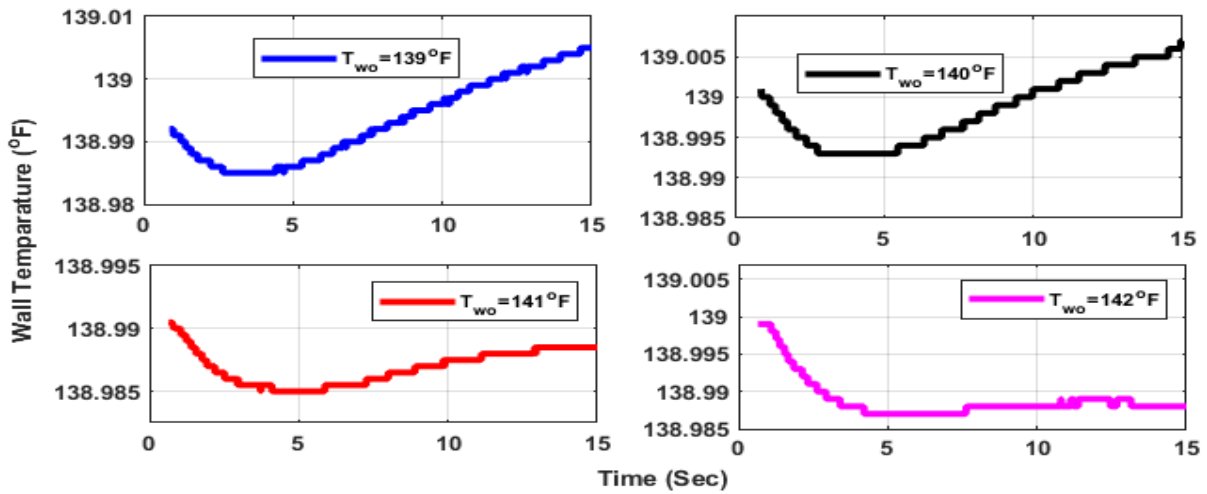


Fig. (8): Variation of wall temperature with time at various initial wall temperature ($\tau_{ws}=3$ sec, $\tau_{wp}=3$ sec, $\tau_w=2$ sec, $V_s=5$ ft/sec).

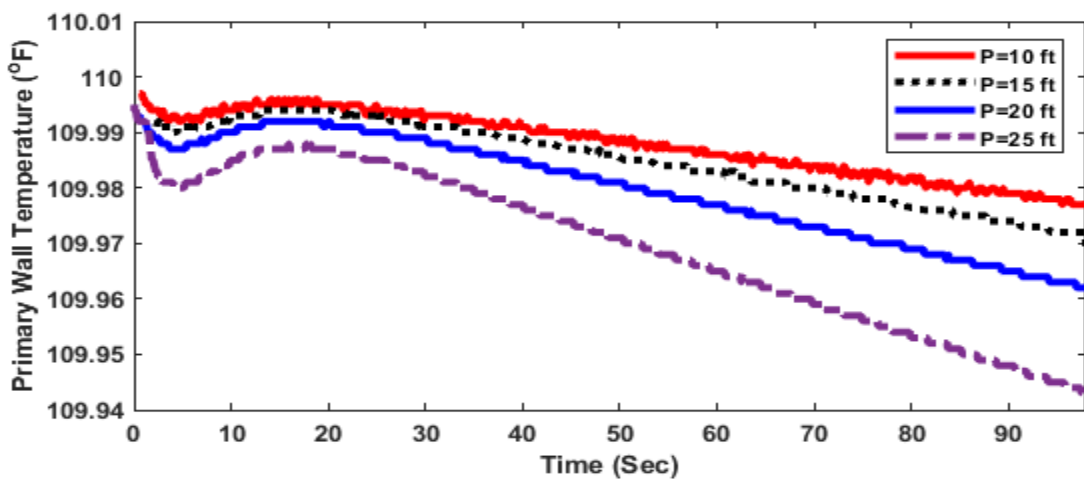


Fig. (9): Variation of primary wall temperature with time at various perimeter ($\tau_{ws}=3$ sec, $\tau_{wp}=3$ sec, $\tau_w=2$ sec, $V_s=5$ ft/sec).

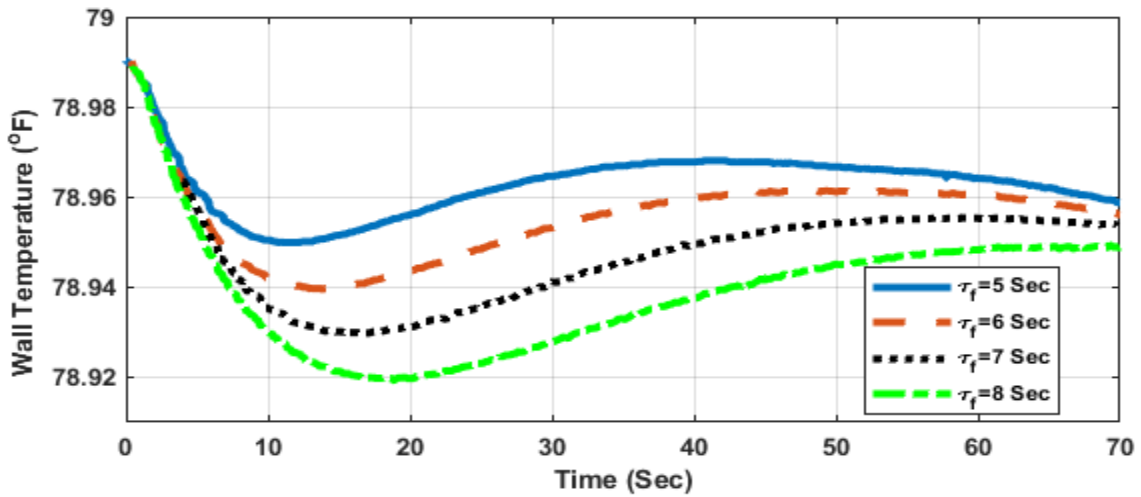


Fig. (10): Variation of primary wall temperature with time at various fluid HT time constant ($\tau_{ws}=3\text{sec}$, $\tau_{wp}=3\text{sec}$, $\tau_w=2\text{sec}$, $V_s=5\text{ft/sec}$).

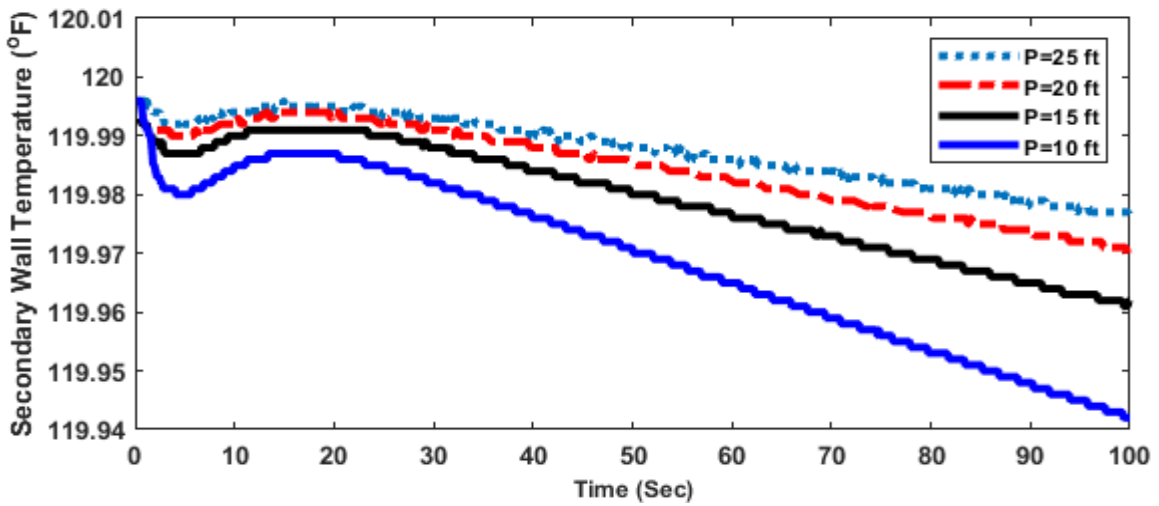


Fig. (11): Variation of secondary wall temperature with time at various perimeter ($\tau_{ws}=3\text{sec}$, $\tau_{wp}=3\text{sec}$, $\tau_w=2\text{sec}$, $V_s=5\text{ft/sec}$).

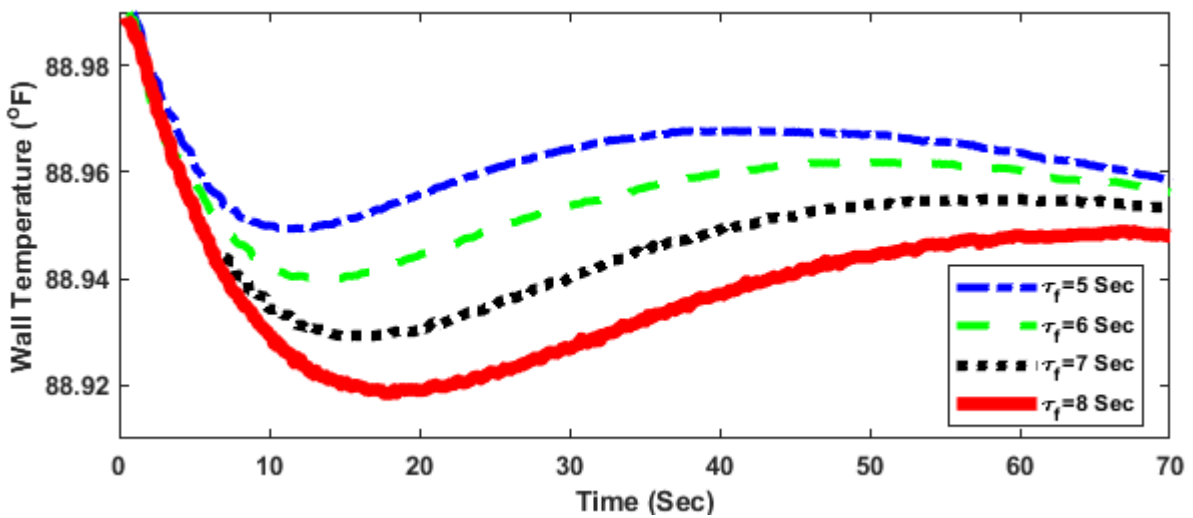


Fig. (12): Variation of secondary wall temperature with time at various fluid HT time constant ($\tau_{ws}=3\text{sec}$, $\tau_{wp}=3\text{sec}$, $\tau_w=2\text{sec}$, $V_s=5\text{ft/sec}$).

4- CONCLUSION

This study presents the exact solutions of the HEX temperature in the pressurized water reactor. The variation of wall temperature with time at various pipe wall heat capacities is analyzed and evaluated. The Variation of wall temperature with time at various fluid HT time constants is presented. The results indicate that the wall temperature of HEX is decreased with increasing time constant of the wall temperature. While the variation of secondary wall temperature increased with increasing time at various fluid HT time constants. Moreover, the variation of the secondary wall temperature with time at various perimeter has been studied and analyzed. Consequently, this study proposed explicit models for wall temperature, primary wall temperature and secondary wall temperature. The proposed models provided the possibilities of variable tuning which are; the pipe wall heat capacities, the fluid HT coefficient, the wall HT coefficient, the fluid HT time constant, the perimeter and the initial wall temperature. The results indicate that the interface between the two fluid passes reduces the transferred temperature depending on the pass parameters. The results show that the convoyed temperature of the fluid is restricted to the wall length and the HEX area is related to the perimeter so, the perimeter changes the behaviors of the HEX within the NPP.

REFERENCES

- [1] C. Y. Xie, H. Z. Tao, W. Li, and J. J. Cheng, "Numerical simulation and experimental investigation of heat pipe heat exchanger applied in residual heat removal system," *Annals of Nuclear Energy*, vol. 133, pp. 568-579, 2019.
- [2] V. Vourganti, "Nonlinear Dynamics Of Heat-Exchanger Tubes Under Crossflow : A Time-Delay Approach," PhD, Department of Mechanical and Aerospace Engineering, Indian Institute of Technology Hyderabad, India, 2020.
- [3] M. El-Sefy, M. Ezzeldin, W. El-Dakhkhni, L. Wiebe, and S. Nagasaki, "System dynamics simulation of the thermal dynamic processes in nuclear power plants," *Nuclear Engineering and Technology*, vol. 51, pp. 1540-1553, 2019.
- [4] T. W. Kerlin and B. R. Upadhyaya, "Chapter 13 - Boiling water reactors," in *Dynamics and Control of Nuclear Reactors*, T. W. Kerlin and B. R. Upadhyaya, Eds., ed: Academic Press, 2019, pp. 167-189.
- [5] M. T. P. K. MURALIMANO HAR, (2009). "Advanced Power Plant Modeling with Applications to the Advanced Boiling Water Reactor and the Heat Exchanger," Master of science, Faculty of Rensselaer Polytechnic Institute, New York, 2009.
- [6] M. M. F. A. Rabbo, A. F. Allah, and M. El-Fawal, "On the Optimal Design of Shell and Tube Heat Exchanger for Nuclear Applications," *Atomic Energy*, pp. 181-195, 1997.
- [7] L. Lovász and I. Boros, "Heat removal possibilities of nuclear containments during a severe accident," *IYCE 2013 - 4th International Youth Conference on Energy*, pp. 1-5, 2013.
- [8] B. W. Huang, G. S. Chen, and C. T. Yu, "Parametric resonance of a fluctuation fluid flow heat exchanger system," *International Journal of Mechanical Sciences*, vol. 146-147, pp. 386-395, 2018.
- [9] M. Ilyas and F. Aydogan, "A new dimensionless thermal hydraulics parameter for the heat exchangers," *Annals of Nuclear Energy*, vol. 118, pp. 154-164, 2018.
- [10] A. H. Abed, S. E. Shcheklein, and V. M. Pakhaluev, "Heat transfer intensification in emergency cooling heat exchanger and dry cooling towers on nuclear power plant using air-water mist flow," *Nuclear Energy and Technology*, vol. 5, pp. 281-287, 2019.
- [11] B. Zohuri, "Heat Pipe Application In Fission Driven Nuclear Power Plant," *International Journal of Earth & Environmental Sciences*, vol. 4, 2019.
- [12] C. T. Inman, "Exploring the Improvement of HTGR Economics with Heat Storage for Variable Electricity Output at Base-Load Operations by," B.Sc in Nuclear Science and Engineering, Nuclear Science and Engineering, MASSACHUSETTS INSTITUTE OF TECHNOLOGY, Massachusetts Institute of Technology, 2019.
- [13] Y. Liu, X. Wang, X. Meng, and D. Wang, "A review on tube external heat transfer for passive residual heat removal heat exchanger in nuclear power plant," *Applied Thermal Engineering*, vol. 149, pp. 1476-1491, 2019.
- [14] B. U. Bae, S. Kim, Y. S. Park, and K. H. Kang, "Experimental investigation on condensation heat

- transfer for bundle tube heat exchanger of the PCCS (Passive Containment Cooling System)," *Annals of Nuclear Energy*, vol. 139, pp. 107285-107285, 2020.
- [15] Z. b. Cai, Z. y. Li, M. g. Yin, M. h. Zhu, and Z. r. Zhou, "A review of fretting study on nuclear power equipment," *Tribology International*, vol. 144, pp. 106095-106095, 2020.
- [16] S. Talebi and N. Norouzi, "Entropy and exergy analysis and optimization of the VVER nuclear power plant with a capacity of 1000 MW using the firefly optimization algorithm," *Nuclear Engineering and Technology*, 2020.
- [17] R. de la Torre, J. L. François, and C. X. Lin, "Assessment of the design effects on the structural performance of the Printed Circuit Heat Exchanger under very high temperature condition," *Nuclear Engineering and Design*, vol. 365, pp. 110713-110713, 2020.
- [18] X. L. Yang, Y. Gong, Q. Tong, and Z. G. Yang, "Failure analysis on abnormal bursting of heat transfer tubes in spiral-wound heat exchanger for nuclear power plant," *Engineering Failure Analysis*, vol. 108, pp. 104298-104298, 2020.
- [19] R. Mehul, "A Research on Heat Exchangers used in Generation-IV Nuclear Reactors," *International Journal of Engineering Research and*, vol. 09, pp. 398-410, 2020.
- [20] E. Martelli, A. Del Nevo, P. Lorusso, F. Giannetti, V. Narcisi, and M. Tarantino, "Investigation of heat transfer in a steam generator bayonet tube for the development of PbLi technology for EU DEMO fusion reactor," *Fusion Engineering and Design*, vol. 159, pp. 111772-111772, 2020.
- [21] M. M. Aslam Bhutta, N. Hayat, M. H. Bashir, A. R. Khan, K. N. Ahmad, and S. Khan, "CFD applications in various heat exchangers design: A review," *Applied Thermal Engineering*, vol. 32, pp. 1-12, 2012/01 2012.
- [22] M. C. Tayal, Y. Fu, and U. M. Diwekar, "Optimal Design of Heat Exchangers: A Genetic Algorithm Framework," *Industrial & Engineering Chemistry Research*, vol. 38, pp. 456-467, 1999/02 1999.
- [23] M. Álvarez-Fernández, L. d. Portillo-Valdés, and C. Alonso-Tristán, "Thermal analysis of closed feedwater heaters in nuclear power plants," *Applied Thermal Engineering*, vol. 68, pp. 45-58, 2014/07 2014.
- [24] M. S. El-Tokhy and I. I. Mahmoud, "Temperature Coupling Analysis Between Nuclear Steam Generators and Heat Exchanger Inside Pressurized Water Reactors," *Nuclear Science and Engineering*, pp. 1-32, 2020.
- [25] D. A. John, "Computational Fluid Dynamics: Chapter 2: Governing Equations of Fluid Dynamics," *Computational Fluid Dynamics*, pp. 15-51, 2009.
- [26] P. K. Muralimanohar, "Advanced Power Plant Modeling With Applications To The Dvanced Boiling Water Reactor And The Heat Exchanger," Master of science, electrical power engineering, Faculty of Rensselaer Polytechnic Institute, 2009.